

D. LEŚNIAK\*, A. WOŹNICKI\*

**EXTRUSION OF AlCuMg ALLOYS WITH SIMULTANEOUS SOLUTION HEAT TREATMENT****WYCISKANIE STOPÓW AlCuMg PRZESYCANYCH NA WYBIEGU PRASY**

In the work, the experiments on extrusion of high-strength aluminium alloys (2014 and 2024) with solution heat treatment on the press were performed. The experimental study describes extrudates microstructure and mechanical properties in dependence on alloy chemical composition, mode of homogenization treatment and temperature-speed extrusion conditions. The optical microscopy and SEM/EDS characterization were supported by DSC analysis, enabling to determine the solidus temperatures of the alloys. The investigations revealed that minimal contents of the main alloy additions (Cu, Mg), high-temperature homogenization and increased extrusion temperatures contributed to achieving high solutioning ratio of the alloys, guarantying improved mechanical properties of the extrudates. The high-temperature homogenization allowed achieving uniform microstructure of ingots with fine particles of intermetallic phases. The significant increase in solidus temperatures of the homogenized alloys enabled more effective solutioning on the run-out table. The maximal permissible metal exit speed was increased and the extrusion force was reduced in comparison to the conventional extrusion technology. The proposed solutions will allow for industrial producing AlCuMg extrudates of improved mechanical properties in the shortened technological cycle with heat treatment on the press.

*Keywords:* extrusion, solution heat treatment, AlCuMg alloys, structure, mechanical properties

W pracy przeprowadzono badania doświadczalne procesu wyciskania wysokowytrzymałych stopów aluminium (2014 i 2024) z jednoczesnym przesycaniem na wybiegu prasy. Studium doświadczalne opisuje strukturę i własności mechaniczne wyciskanych prętów, w zależności od składu chemicznego stopu, sposobu homogenizacji oraz prędkościowo-temperaturowych warunków procesu wyciskania. Badania strukturalne z wykorzystaniem mikroskopii optycznej i SEM uzupełniono badaniami kalorymetrycznymi, które pozwoliły na wyznaczenie temperatury solidusu stopów. Badania wykazały, że minimalizacja zawartości głównych składników stopowych (Cu i Mg), wysokotemperaturowa homogenizacja wlewków oraz wyciskanie w wysokich temperaturach (wyższych niż standardowe), przyczynia się do uzyskania wysokiego stopnia przesycenia stopów na wybiegu prasy, gwarantującego otrzymanie wysokich własności mechanicznych wyrobów. Wysokotemperaturowa homogenizacja pozwoliła na uzyskanie jednorodnej struktury wlewków z drobnymi wydzieleniami faz międzymetalicznych. Znaczny wzrost temperatury solidusu homogenizowanych stopów umożliwił bardziej efektywne przesycanie na wybiegu prasy. Wykazano możliwość zwiększenia maksymalnej dopuszczalnej prędkości wypływu metalu z otworu matrycy i obniżenia siły w procesie wyciskania, w porównaniu z konwencjonalną technologią wyciskania tych stopów. Proponowane rozwiązania pozwolą na produkcję przemysłową kształtowników AlCuMg o wysokich własnościach mechanicznych, w jednym skróconym cyklu technologicznym połączonego wyciskania z obróbką cieplną.

**1. Introduction**

Standard extrusion technology for high-strength aluminium alloys in T6 temper allows producing profiles of simple geometrical shapes. This technology needs an additional heating of the extrudates to solution temperature what increases manufacturing costs and worsens the product quality by unfavourable grain growth and shape distortions. Dixon [1] has indicated the main limitations of extrusion of AlCuMg alloys, such as low melt-

ing point of the alloys and a coarse-grained structure of extrudates produced during conventional solutioning. Senderski et al. [2] have demonstrated that applying extrusion with solution heat treatment on the press reduces or even prevents the formation of peripheral coarse grain in extrudates of certain AlCuMg alloys. The same conclusions can be drawn from the work of Leśniak [3], in which the water solution heat treatment on the press of 2014 alloy allowed eliminated the peripheral coarse grain observed in case of the conventional T6 extru-

\* AGH UNIVERSITY OF SCIENCE AND TECHNOLOGY, FACULTY OF NONFERROUS METALS, 30-059 KRAKÓW, 30 MICKIEWICZA AV., POLAND

sion technology. Shepard [4] has found that some of the 2xxx alloys can be press-quenched and aged to the high mechanical properties levels, provided that the extrusion temperature is sufficiently high. However, in this case the melting temperature of these alloys may be exceeded. Xu et al. [5] has demonstrated that solution heat treatment followed by water quenching, enhanced by means of increasing solutioning temperature from 500°C to 510°C, improves the yield strength of 2024 alloy.

The extrusion with a solution heat treatment on the press (in T5 temper) is more and more frequently technology applied in production practice, allowing significant shortening of the technological cycle and reduction of production costs. This technology is commonly used in the case of 6xxx alloys and some 7xxx alloys, but is still not implemented to industrial practice for 2xxx alloys. A special cooling system on the press run-out must be installed as presented in the work of Kramer [6]. However, the relatively large distance between the die opening and quenching zone on the run-out table and low extrusion speeds, result in incomplete solution of the AlCuMg alloys on the press. Moreover, these alloys have a narrow solvus-solidus range and there is a risk of exceeding the melting temperature of the alloy, as demonstrated in work of Totten and MacKenzie [7].

In order to achieve the required mechanical properties of the 2xxx profiles in T5 temper, the ingots for extrusion with solution heat treatment on the press should be characterized by:

- the presence of fine hardening particles in their structure, which would be fully dissolved during extrusion,
- as low as possible flow stress, to increase the extrusion speed and reduce the time required to transport

the profile from the die to quenching installation on the press. This is essential for retaining the all alloy additions in the solid solution.

The above-mentioned conditions have to be taken into consideration during evaluation of the homogenization parameters. The heating rate to homogenization temperature should be relatively low. Otherwise, due to the slow diffusion rate of copper in aluminium, the local concentrations of alloying additions can cause melting of the alloy in surroundings of the unsolved particles. The temperature of homogenization should exceed the solvus temperature, to provide the full dissolution of hardening phase particles, but should be below the lowest eutectic temperature of the alloy to avoid melting. Thus, in the industrial practice, the multi-stage homogenization schemes are applied, in which the eutectic temperature is exceeded in the last stage of the process. Dissolution of secondary phases, taking place during homogenization, causes a gradual increment of the alloy solidus temperature (from unequilibrium to equilibrium), and allows to rise the annealing temperature successively (Fig. 1).

It is commonly known, that at higher temperature the homogenization runs faster. Leśniak et al. [8] revealed that the high-temperature homogenization of 2014 and 2024 alloys, performed close to the solidus temperatures, allowed obtaining uniform microstructure with fine particles of the intermetallic phases (which can be easily dissolved within the deformation zone during extrusion), without the formation of overheated microstructures. Higher homogenization temperatures can be applied for alloys with minimal additions content (Cu, Mg). Goncalves et al. [9] has shown that optimum hot workability of 2014 alloy can be achieved by use of slow cooling after homogenization.

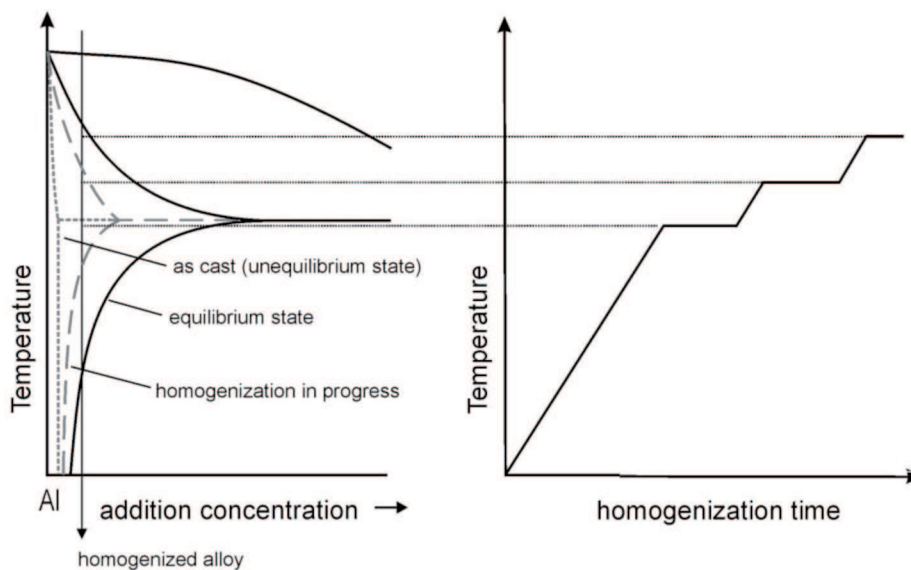


Fig. 1. Temperature-time dependence during homogenization of AlCuMg alloys

The aim of this work was to analyse the structure and mechanical properties of AlCuMg extrudates in T5 temper – for alloys with minimized contents of the main alloy additions (Cu and Mg), subjected to high-temperature homogenization, and increased extrusion temperatures.

## 2. High-temperature homogenization

The high-temperature homogenization of 2014 and 2024 alloys with the lowest permissible contents of the main alloying additions Cu and Mg (signed as A and C alloys in Tables 1 and 3) was proposed in the research. A special treatment procedure consisted in a gradual heating up to homogenization temperature close to the solidus temperature ( $T_H = 510^\circ\text{C}$ ), short holding of material at the homogenization temperature and slow cooling down after homogenization.

Homogenization of 2024 and 2024 alloys with the highest permissible contents of Cu and Mg (signed as B and D alloys in Tables 2 and 4) at standard conditions ( $490^\circ\text{C}/12\text{h}$  for 2014 alloy and  $500^\circ\text{C}/11\text{h}$  for 2024 alloy) was also performed for comparison.

The schemes of the standard homogenization and the high-temperature treatment are shown in Fig. 2. The chemical compositions of all the alloys (in the range of the proper standard [11]) are shown in Tables 1-4. In further analysis, the alloys with the lowest and highest permissible content of Cu and Mg are to be called “low alloyed” and “high alloyed” respectively.

TABLE 1

Chemical composition of 2014 alloy with the lowest permissible content of Cu and Mg (A alloy)

Element	Cu	Mg	Mn	Si	Fe	Zn	Ti
Weight %	4.00	0.24	1.19	1.15	0.10	0.028	0.03

TABLE 2

Chemical composition of 2014 alloy with the highest permissible content of Cu and Mg (B alloy)

Element	Cu	Mg	Mn	Si	Fe	Zn	Ti
Weight %	5.00	0.76	1.17	1.11	0.10	0.028	0.03

TABLE 3

Chemical composition of 2024 alloy with the lowest permissible content of Cu and Mg (C alloy)

Element	Cu	Mg	Mn	Si	Fe	Zn	Ti
Weight %	3.56	1.23	0.90	0.06	0.12	0.028	0.03

TABLE 4

Chemical composition of 2024 alloy with the highest permissible content of Cu and Mg (D alloy)

Element	Cu	Mg	Mn	Si	Fe	Zn	Ti
Weight %	4.90	1.77	0.89	0.06	0.12	0.028	0.03

The optical microscope (Olympus GX51) was used to observe microstructure of the alloys submitted to different heat treatment procedures. Figures 3-4 present the microstructures of 2014 and 2024 alloys with both the lowest and highest permissible content of the main alloy additions (Cu, Mg) – after casting and different homogenization conditions.

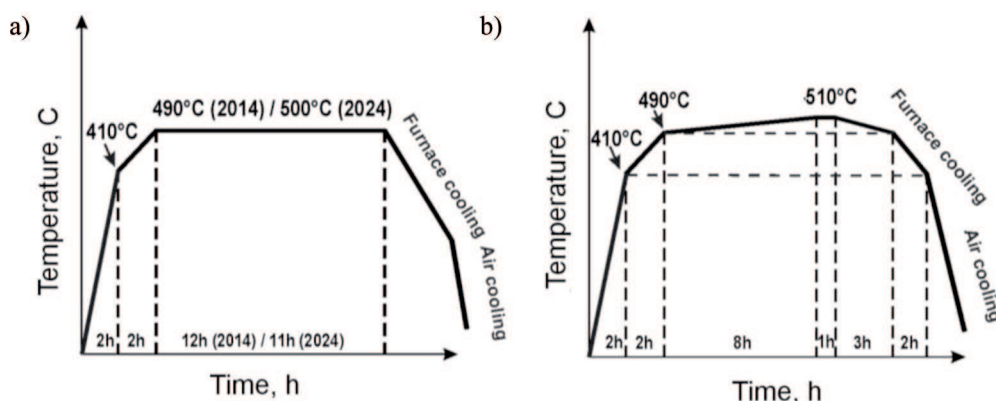


Fig. 2. Schemes of the homogenization procedures for 2014 and 2024 alloys (a) standard homogenization (b) high-temperature treatment

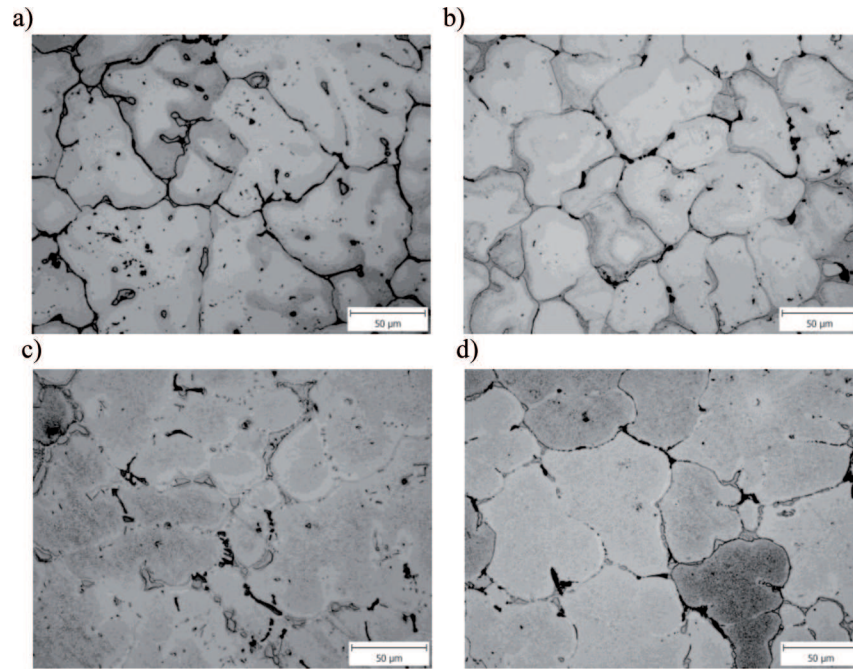


Fig. 3. Microstructures of cast and homogenized 2014 alloy with the extreme contents of Cu and Mg (a) 2014 low alloyed (A alloy), as-cast (b) 2014 high alloyed (B alloy), as-cast (c) 2014 low alloyed (A alloy), homogenized 510°C/9h (d) 2014 high alloyed (B alloy), homogenized 490°C/12h

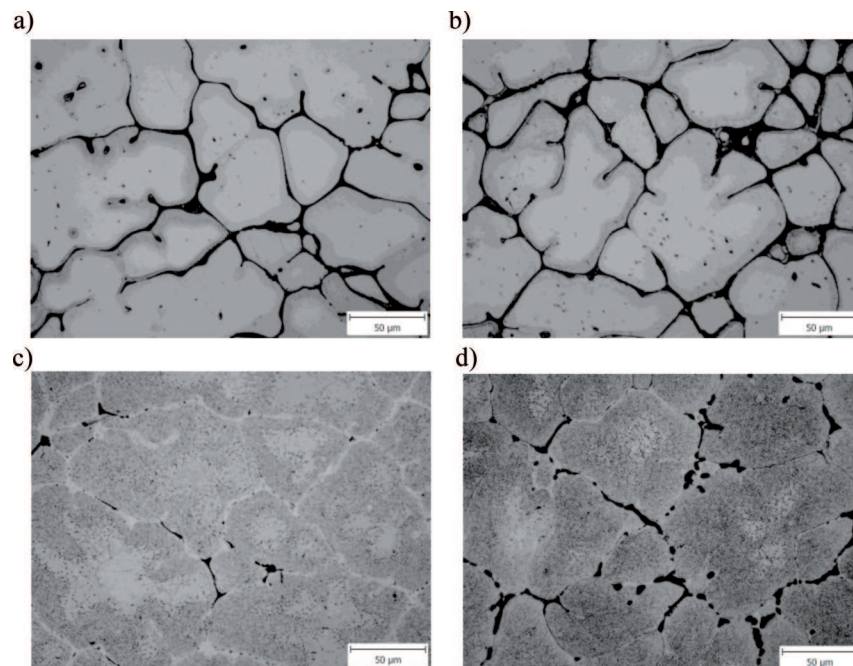


Fig. 4. Microstructures of cast and homogenized 2024 alloy with the extreme contents of Cu and Mg (a) 2024 low alloyed (C alloy), as-cast (b) 2024 high alloyed (D alloy), as-cast (c) 2024 low alloyed (C alloy), homogenized 510°C/9h (d) 2024 high alloyed (D alloy), homogenized 500°C/11h

The visible is an undesirable microstructure with big particles of interdendritic phases produced during the casting (Figs 3a-b and 4a-b). Figures 3d and 4d show that application of conventional homogenization after casting leads to certain improvement of the microstructure. More

uniform structure with smaller particles of intermetallic phases is produced. The minimizing content of the alloy additions and conducting homogenization at the high temperatures contribute to formation of the uniform microstructure with fine intermetallic particles (Figs 3c and



4c), which can be easily dissolved within the deformation zone during extrusion. Because of such ingots treatment, the more effective solution heat treatment at the press output and increased strength properties of extrusions in T5 temper are expected.

### 3. Differential scanning calorimetry analysis

The samples from cast and heat-treated materials were taken for the differential scanning calorimetry (DSC) analysis. The DSC was done in a calorimeter using 5 mm diameter discs, which were 3 mm thick, heated at 20°C/min. This allowed to determine the solidus temperatures of the tested alloys. The results for the cast and homogenized 2014 and 2024 alloys with extreme contents of Cu and Mg are shown in Fig. 5.

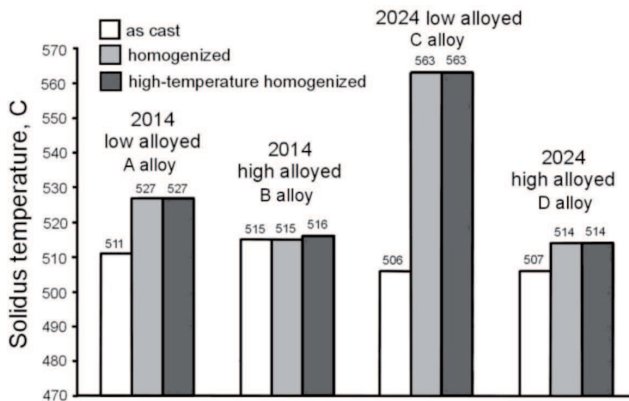


Fig. 5. Solidus temperatures of cast and homogenized 2014 and 2024 alloys

For the alloys with the highest contents of Cu and Mg, for which the solidus temperatures are relatively low (515°C for 2014 alloy and 507°C for 2024 alloy), there is a risk of exceeding the limit solidus temperature of the alloy during extrusion with simultaneous solution heat treatment. This can result in forming of the over-melts in the alloy. The reduced content of Cu and Mg, contributed to the considerable increase in the solidus temperatures for the homogenized alloys, especially for 2024 alloy, where it rose from 506°C up to 563°C. In consequence, extrusion could be performed at the higher temperature what facilitated the solutioning on the press. The increase in the solidus temperature is also beneficial from the ingot heat treatment point of view. This makes possible to use a higher final temperature of homogenization to completely dissolve particles of the formed phases.

### 4. Extrusion with solution heat treatment

The laboratory extrusion with solution heat treatment at the press output was carried out in a 3 MN direct press (vertical), equipped with a system for measuring the extrusion force and laser pyrometer Optris CT for precise non-contact temperature measurement of metal leaving the die opening. The rods of 10 mm in diameter were extruded into the water container located at a distance of 100 mm from the die opening. The schemes of the extrusion process and tools assembly used in experiments are presented in Fig.6a-b.

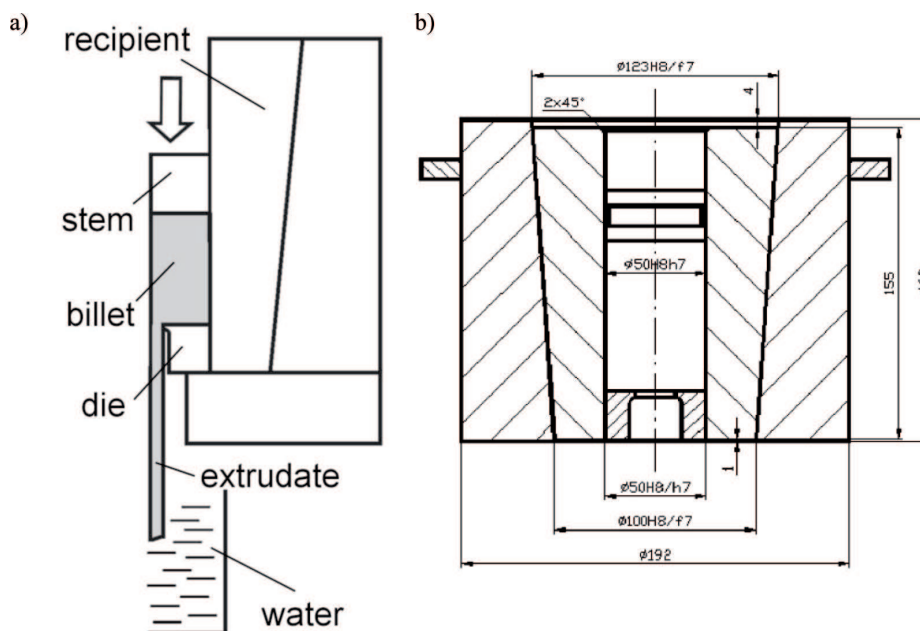


Fig. 6. Extrusion process and tools (a) scheme of extrusion into the water (b) tools assembly

Extrusion trials with simultaneous solution heat treatment were performed for the high-temperature homogenized (510°C/9h) 2014 and 2024 alloys with the lowest permissible content of Cu and Mg (A alloy in Table 1 and C alloy in Table 3), at relatively high extrusion temperatures and varying metal exit speeds. The billets of 50 mm in diameter and 70 mm in length were preheated for extrusion up to 500°C.

The conventional T6 extrusion of the homogenized 2014 and 2024 alloys with the highest permissible contents of Cu and Mg (B alloy: Table 2 and D alloy: Table 4) was carried out for comparison. All the extrusion conditions are presented in Tables 5 and 6. The heat treatment conditions are presented in Table 7.

TABLE 5  
Conditions of the extrusion process of AlCuMg alloys with solution heat treatment on the press

Extrusion T5	2014 alloy	2024 alloy
Billets	Ø50×70 mm High-temperature homogenized at 510°C/9h	
Extrudates (rods)	Ø10 mm	
Extrusion ratio, $\lambda$	25	
Metal exit speed, $V_1$	1, 2.5 m/min	0.75, 2 m/min
Billet and tools temperature, $T_0$	500°C	
Friction conditions	Sticking	

TABLE 6  
Conditions of the conventional T6 extrusion process of AlCuMg alloys

Extrusion T6	2014 alloy	2024 alloy
Billets	Ø50×70 mm Homogenized 490°C/12h	Ø50×70 mm Homogenized 500°C/11h
Extrudates (rods)	Ø10 mm	
Extrusion ratio, $\lambda$	25	
Metal exit speed, $V_1$	2 m/min	1.5 m/min
Billet and tools temperature, $T_0$	450°C	420°C
Friction conditions	Sticking	

TABLE 7  
Parameters of solution heat treatment (conventional) and aging of AlCuMg extrudates

Heat treatment	2014 alloy	2024 alloy
Solution heat treatment	503°C/1h	490°C/1h
Aging	175°C/11h	190°C/12h

## 5. Surface quality of extrudates

First, the extruded rods were examined for surface quality. Fig. 7 presents the billet rests and the end part of the rods received in extrusion of the 2014 and 2024 alloys, for different chemical compositions, extrusion temperature-speed conditions, and the solution heat treatment.

The increasing metal exit speed while extruding low-alloyed AlCuMg with solution heat treatment on the press did not affect negatively the surface quality of extrudates, even for relatively high extrusion temperature of 500°C (Figs 7c and 7f). For the both analyzed alloys, the increase in maximal permissible metal exit speed (2.5 m/min for 2014 alloy and 2 m/min for 2024 alloy) was about of 25%, in comparison to values obtained for the conventional T6 extrusion. This allows reducing the time needed for extrusions to reach the cooling zone in the water-wave installation, and to perform the solutioning effectively. In addition, higher exit temperature accelerates dissolution of the hardening phases' particles.

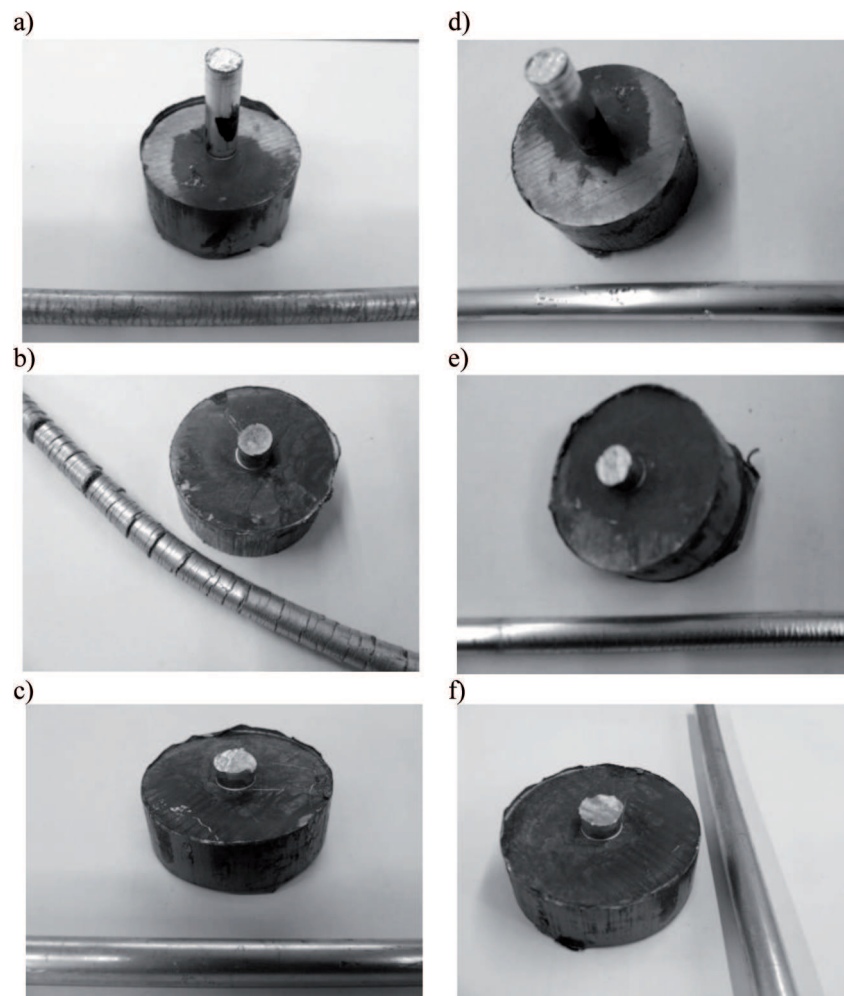


Fig. 7. The billet rests and end part of rods received in extrusion of 2014 alloy (a-c) and 2024 alloy (d-f) (a) 2014 high alloyed (B alloy) extruded in T6 temper,  $T_0 = 450^\circ\text{C}$ ,  $V_1 = 2$  m/min (b) 2014 high alloyed (B alloy) extruded in T6 temper,  $T_0 = 500^\circ\text{C}$ ,  $V_1 = 2$  m/min (c) 2014 low alloyed (A alloy) extruded with solution heat treatment on the press,  $T_0 = 500^\circ\text{C}$ ,  $V_1 = 2.5$  m/min (d) 2024 high alloyed (D alloy) extruded in T6 temper,  $T_0 = 420^\circ\text{C}$ ,  $V_1 = 1.5$  m/min (e) 2024 high alloyed (D alloy) extruded in T6 temper,  $T_0 = 500^\circ\text{C}$ ,  $V_1 = 1.5$  m/min (f) 2024 low alloyed (C alloy) extruded with solution heat treatment on the press,  $T_0 = 500^\circ\text{C}$ ,  $V_1 = 2$  m/min

## 6. Microstructure of extruded alloys

The extrudates were submitted to the structural observations using the optical microscopy and SEM characterization with EDS microanalysis. The microstructures of extruded rods in longitudinal section are presented in Figs 8-9 (2014 alloy) and 10-11 (2024 alloy). The observation with the use of the SEM/BSE techniques and EDS microanalysis showed that in case of T5 extrusion of the low alloyed 2014, two types of particles were found in extrudates structure: the elongated bright particles, containing mainly Al and Cu, assumed to be  $\text{Al}_2\text{Cu}$  phase and grey ones, containing Al, Mn, Cu, Si and Fe (Fig. 8). The microstructure of the high-alloyed 2014 extrudates in T6 temper, contains the similar particles and additionally, the fewer dark-grey particles, containing Al, Si, Mg and Cu (Fig. 9). The number and size of particles in the microstructure of 2014 extrudates in T5

and T6 temper are very similar, whereas in the case of the 2024 alloy in T5 and T6 tempers the microstructures are essentially different.

In the microstructure of the low-alloyed 2024 rods, quenched from the extrusion temperature, the inhomogeneous particles containing Al, Cu, Mn, Fe and Mg are present (Fig. 10). In case of the 2024 alloy with high additions content, a considerably higher number of particles of about 10 nm, containing Al, Cu and Mg are observed. They are visible as bright particles in Fig. 11 and were identified as undissolved  $\text{Al}_2\text{CuMg}$  phase. The dark, smaller particles contain Al, Cu, Mn, Mg and Fe.

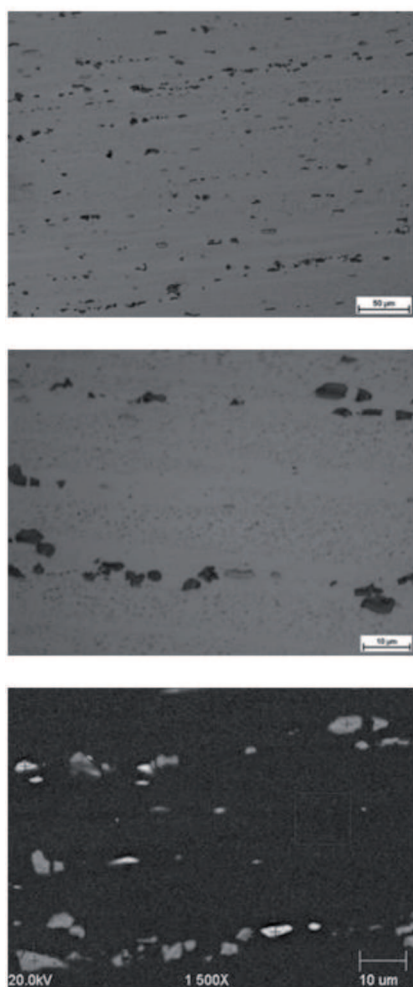
Fig. 12 shows a comparison of the main additions concentration in matrix, and their total content in the alloys. Copper and magnesium are present in matrix in the form of very fine hardening precipitates. In case of the 2014 alloy (Fig. 12a), Cu content in matrix is in proportion with total Cu content in alloy. The concentra-

tion of magnesium in the matrix of highly alloyed 2014 is about 50% higher than in low-alloyed 2014 matrix, whereas total magnesium content in high-alloyed 2014 is three times higher than in low-alloyed 2014 variant. It was found that with increase of Cu and Mg content in the matrix the higher strength properties of extrudates were obtained.

The concentration of Cu in matrix of the highly alloyed 2024 is about 10% higher in comparison with that in the low-alloyed case, whereas total Cu concentration in high-alloyed 2024 is about 30% higher than in low-alloyed variant (Fig. 12b). The concentration of magnesium in the matrix of highly alloyed 2024 is a little lower than that in the low-alloyed one. This means

that in the highly alloyed 2024 extrudates', the substantial amount of Cu and Mg is present in form of coarse particles. Thus, in the case of the 2024 alloy there is no relationship between the concentration of additions in the alloys and in the matrix. Therefore, the strength properties of the 2024 alloy are not dependent on the concentrations of the alloying additions.

Generally, for alloys with minimal additions content, a low amount of unsolved particles of hardening phases was stated in the structure of extrusions quenched on the press. Referring to the high strength properties obtained for these extrusions after aging this proves the high solutioning ratio of the alloys.



#### Particle 1 analysis

Element	Concentration, wt%	Error 2 $\sigma$
Mg	0,1	0,1
Al	60,8	1,6
Si	10,3	0,9
Mn	19,7	1,4
Fe	3,7	0,6
Cu	5,0	1,0
Zn	0,2	0,2

#### Particle 2 analysis:

Element	Concentration, wt%	Error 2 $\sigma$
Mg	0,1	0,1
Al	58,1	1,8
Si	0,7	0,2
Ti	0,2	0,1
Fe	0,1	0,1
Cu	40,4	2,8
Zn	0,3	0,3

#### Particle 3 analysis:

Element	Concentration, wt%	Error 2 $\sigma$
Mg	0,4	0,1
Al	68,6	1,7
Si	0,6	0,2
Ti	0,1	0,1
Mn	0,1	0,1
Fe	0,1	0,1
Cu	30,0	2,1
Zn	0,2	0,2

#### Particle 4 analysis:

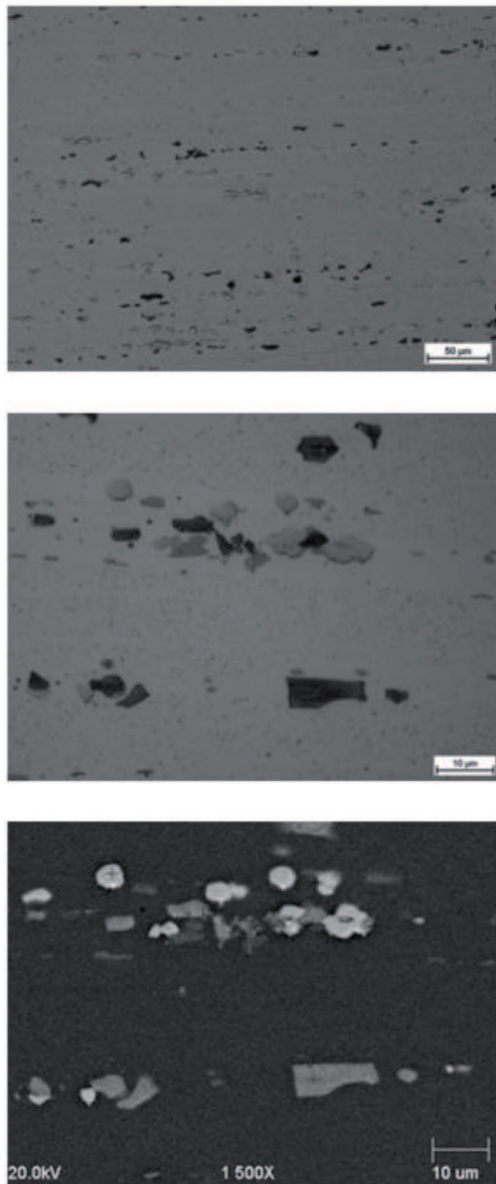
Element	Concentration, wt%	Error 2 $\sigma$
Mg	0,2	0,1
Al	64,0	1,6
Si	8,6	0,8
Ti	0,1	0,1
Mn	17,7	1,3
Fe	3,9	0,6
Cu	5,3	1,0

#### Area 5 analysis:

Element	Concentration, wt%	Error 2 $\sigma$
Mg	0,3	0,1
Al	95,7	1,7
Si	0,2	0,1
Ti	0,2	0,1
Mn	0,2	0,1
Fe	0,2	0,1
Cu	2,7	0,7
Zn	0,5	0,3

Fig. 8. Microstructures of T5 extrusions from 2014 low alloyed (A alloy)



**Particle 1 analysis:**

Element	Concentration, wt%	Error 2 $\sigma$
Al	60,0	1,7
Si	9,4	0,9
Ti	0,1	0,1
Mn	20,5	1,5
Fe	3,2	0,6
Cu	6,5	1,2
Zn	0,2	0,2

**Point 2 analysis:**

Element	Concentration, wt%	Error 2 $\sigma$
Mg	0,2	0,1
Al	56,8	1,8
Si	0,7	0,2
Ti	0,3	0,1
Mn	0,1	0,1
Fe	0,1	0,1
Cu	41,5	2,7
Zn	0,4	0,3

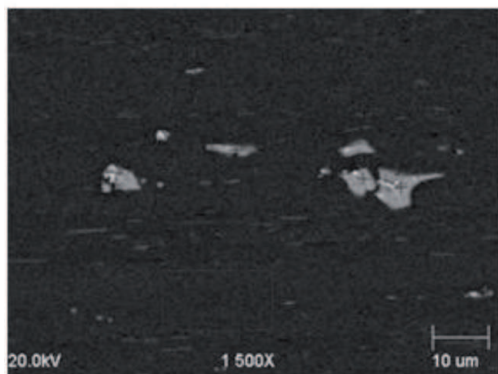
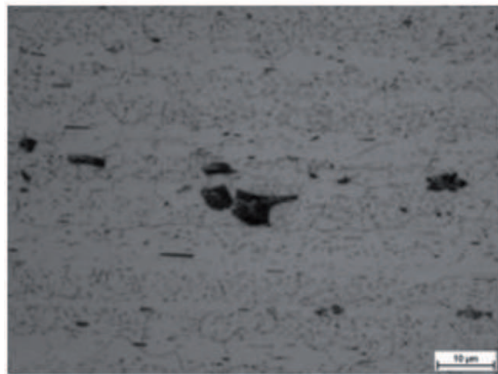
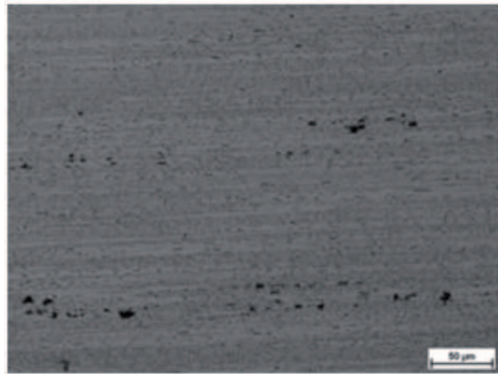
**Particle 3 analysis:**

Element	Concentration, wt%	Error 2 $\sigma$
Mg	11,4	0,6
Al	60,2	1,6
Si	19,0	1,2
Ti	0,1	0,1
Mn	0,3	0,2
Fe	0,2	0,1
Cu	8,7	1,3
Zn	0,1	0,1

**Particle 4 analysis:**

Element	Concentration, wt%	Error 2 $\sigma$
Mg	8,7	0,5
Al	68,1	1,6
Si	14,9	1,1
Ti	0,1	0,1
Mn	0,2	0,1
Fe	0,2	0,1
Cu	7,6	1,2
Zn	0,3	0,3

Fig. 9. Microstructures of T6 extrusions from 2014 high alloyed (B alloy)

**Particle 1 analysis:**

Element	Concentration, wt%	Error 2 $\sigma$
Mg	0,1	0,1
Al	60,0	1,9
Si	0,1	0,1
Ti	0,1	0,1
Mn	12,7	1,2
Fe	7,7	1,0
Cu	19,0	2,1
Zn	0,4	0,3

**Particle 2 analysis:**

Element	Concentration, wt%	Error 2 $\sigma$
Mg	0,2	0,1
Al	58,0	1,8
Si	0,6	0,2
Ti	0,1	0,1
Mn	10,8	1,0
Fe	7,0	0,9
Cu	22,9	2,2
Zn	0,3	0,3

**Particle 3 analysis:**

Element	Concentration, wt%	Error 2 $\sigma$
Mg	1,1	0,2
Al	76,4	1,8
Si	0,1	0,1
Ti	0,2	0,1
Mn	5,4	0,7
Fe	4,6	0,7
Cu	12,0	1,5
Zn	0,3	0,3

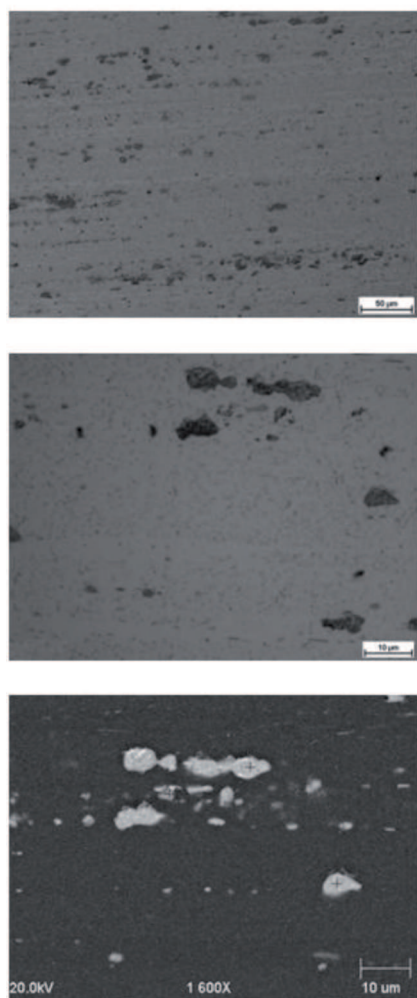
**Particle 4 analysis:**

Element	Concentration, wt%	Error 2 $\sigma$
Mg	1,1	0,2
Al	80,5	1,7
Si	0,1	0,1
Ti	0,1	0,1
Mn	2,1	0,4
Fe	2,5	0,5
Cu	13,2	1,5
Zn	0,4	0,3

**Area 5 analysis:**

Element	Concentration, wt%	Error 2 $\sigma$
Mg	1,6	0,2
Al	94,2	1,7
Si	0,1	0,1
Ti	0,1	0,1
Mn	0,6	0,2
Fe	0,2	0,2
Cu	2,1	0,6
Zn	1,1	0,5

Fig. 10. Microstructures of T5 extrusions from 2024 low alloyed (C alloy)



Particle 1 analysis:

Element	Concentration, wt%	Error 2σ
Mg	13,3	1,0
Al	43,9	1,8
Si	0,1	0,1
Ti	0,2	0,1
Mn	0,5	0,2
Fe	0,2	0,1
Cu	41,6	3,0
Zn	0,3	0,3

Particle 2 analysis:

Element	Concentration, wt%	Error 2σ
Mg	0,9	0,2
Al	76,4	1,8
Si	0,1	0,1
Ti	0,4	0,2
Mn	11,1	1,0
Fe	0,8	0,3
Cu	10,0	1,3
Zn	0,2	0,2

Area 3 analysis:

Element	Concentration, wt%	Error 2σ
Mg	1,4	0,2
Al	95,0	1,7
Ti	0,2	0,1
Mn	0,6	0,2
Fe	0,1	0,1
Cu	1,7	0,5
Zn	1,0	0,5

Particle 4 analysis:

Element	Concentration, wt%	Error 2σ
Mg	13,2	1,0
Al	43,1	1,8
Si	0,3	0,2
Ti	0,1	0,1
Mn	0,2	0,1
Fe	0,2	0,1
Cu	42,4	3,0
Zn	0,5	0,4

Fig. 11. Microstructures of T6 extrusions from 2024 high alloyed (D alloy)

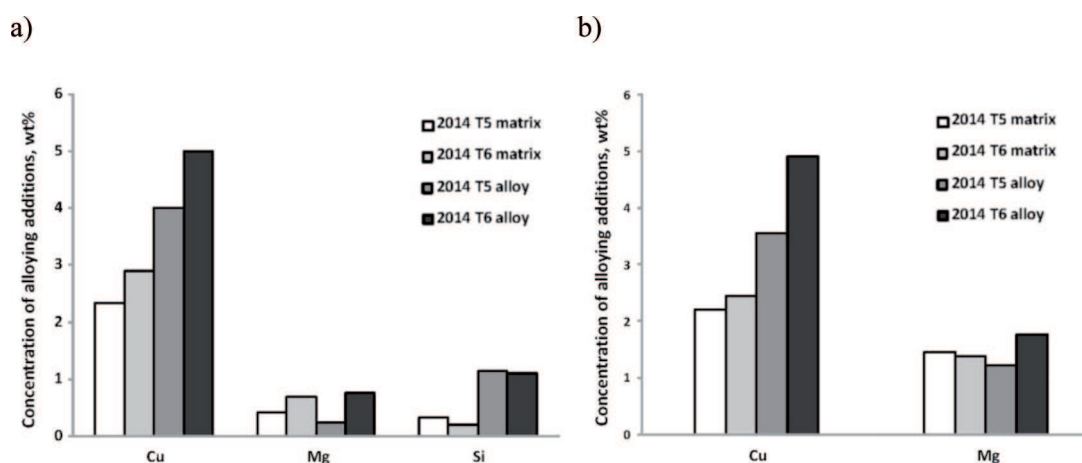


Fig. 12. Comparison of main additions concentrations in matrixes and their total content in the alloys

## 7. Mechanical properties of extrudates

The mechanical testing was carried out on universal Instron 4484 strength machine. Brinell hardness was obtained on the Instron-Wolpert tester. The HB hardness

values were measured in the front-end and back-end of extrudates. Figs 13-14 present the mechanical properties ( $R_{0,2}$ ,  $R_m$ ,  $A_{10}$ , HB) of 2014 and 2024 alloys extruded in T5 and T6 tempers.



The high strength properties were obtained for the alloys with minimal possible content of Cu and Mg (Fig. 13), extruded in T5 temper: the yield stress  $R_{0,2}$  is of 432-445 MPa for 2014 and 366-396 MPa for 2024. The ultimate tensile strength  $R_m$  is of 485-507 MPa for 2014 and is by 5-10% lower than that obtained in the T6 temper (536 MPa). The ultimate tensile strength of the 2024 alloy in T5 temper was of 484-489 MPa and was slightly higher than that in T6 temper (479 MPa). The relatively good ductility was obtained for the alloys in T5 temper:  $A_{10} = 7.1-7.2\%$  (2014) and 6.1-8.4% (2024). In the case of 2014 alloy, the elongation  $A_{10}$  was about 7% and was higher by about 30% to that obtained in T6 temper (4.9%).

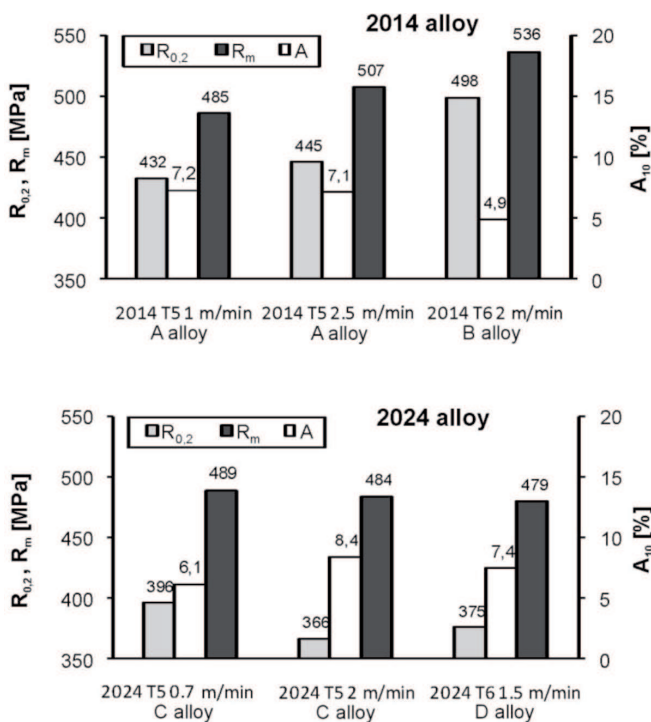


Fig. 13. Yield stress  $R_{0,2}$ , tensile strength  $R_m$ , and elongation  $A_{10}$  of 2014 and 2024 alloys extruded in T5 and T6 tempers

There were no significant differences in hardness values of 2014 and 2024 rods extruded in T5 and T6 tempers (Fig. 14). In general, HB hardness values for rods extruded in T5 temper (135-145 HB for 2014 and 127-130 for 2024) were a little lower than that in T6 temper: 146 HB for 2014 and 134 for 2024 relatively. Obtained mechanical properties of AlCuMg alloys extruded in T5 temper meet requirements of the standard [12].

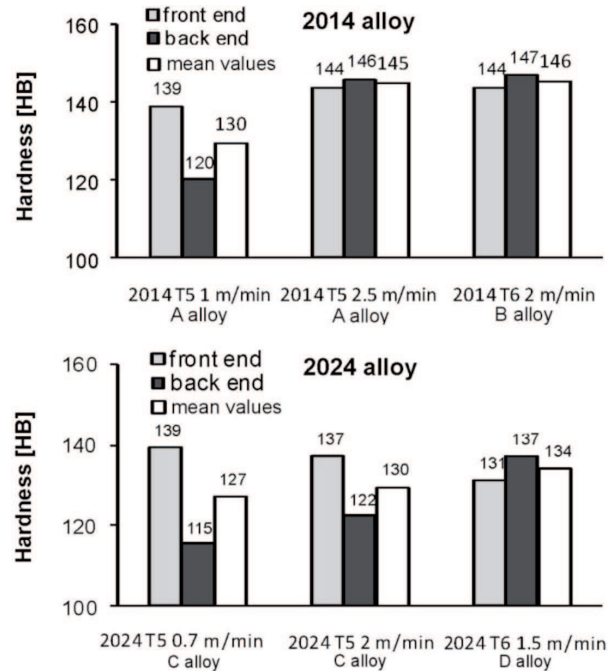


Fig. 14. Hardness HB of 2014 and 2024 alloys extruded in T5 and T6 tempers

## 8. Extrusion force

The process force was measured during extrusion of the analyzed alloys with solution heat treatment at the press output. The decreasing content of the main alloying additions and the relatively high extrusion temperature of 500°C, resulted in reduction of the extrusion force for the both investigated alloys, compared to the conventional T6 extrusion process – 25% for 2014 alloy and 40% for 2024 alloy (fig. 15).

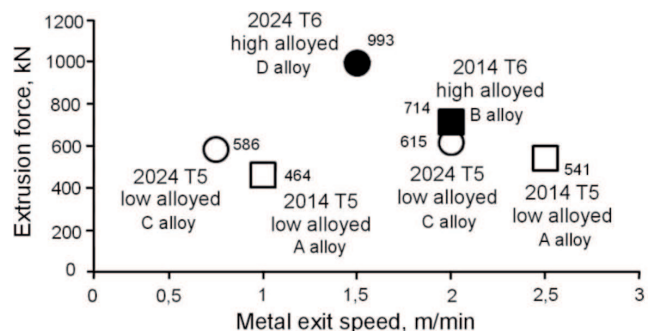


Fig. 15. Dependence of extrusion force on metal exit speed for 2014 and 2024 alloys

## 9. Conclusions

Based on performed extrusion trials of the high-strength 2014 and 2024 alloys with the simulta-



neous solution heat treatment, the following conclusions can be drawn:

1. Minimized contents of the main alloy additions (Cu, Mg), the high-temperature homogenization and increased extrusion temperatures contribute to achieving improved mechanical properties of extrudates.
2. High-temperature homogenization of the low-alloyed ingots formed uniform microstructure, containing fine particles, which can be easily dissolved in the deformation zone during extrusion. This resulted in higher extrusion speed and improved process effectiveness.
3. Reduced contents of the alloying additions Cu and Mg, led to the considerable increase in solidus temperatures of the alloys. In consequence, it was possible to perform the extrusion process at relatively high temperatures and higher exit speed, what facilitated solution heat treatment on the press.
4. In the case of minimal possible contents of Cu and Mg in the alloys and high extrusion temperatures, the extrusion force is decreased, what is of great importance while extruding the hard-deformable aluminum alloys.
5. The proposed solutions will allow industrial producing of AlCuMg extrudates of improved mechanical properties, with reduced both duration of process and production costs.

#### REFERENCES

- [1] K. Laue, H. Stenger, Extrusion, ASME, Metals Park, Ohio, 1981.
- [2] ASM Handbook: Aluminum and Aluminum Alloys, ASM International, 1993.
- [3] B. Dixon, 2000. Extrusion of 2xxx and 7xxx alloys. In: The Aluminum Association & Aluminum Extruders Council, Proceedings of the 7th International Aluminum Extrusion Technology Seminar ET'2000, Chicago, USA, pp. 281-294.
- [4] J. Senderski, L. Pierewicz, B. Plonka, Technology, devices and control of the solution heat treatment process on the press of extruded sections 2xxx and 6xxx. *Ores and Metals* **47**, 284-288 (2002).
- [5] D. Leśniak, Structure and mechanical properties of extruded AlCuMg sections in T5 temper. *Archives of Metallurgy and Materials* **54**, 4, 1135-1145 (2009).
- [6] C. Kramer, Intensive Cooling of Light Metal Alloy Extrusion by Air and Water. In: The Aluminum Association & Aluminum Extruders Council, Proceedings of the 7th International Aluminum Extrusion Technology Seminar ET'2000, Chicago, USA, 397-407 (2000).
- [7] G. E. Totten, D.S. MacKenzie, Physical Metallurgy and Processes, In: Handbook of Aluminum vol. 1 (Eds.: Totten, G.E. & MacKenzie, D.S.), Marcal Dekker, 385-480 (2003).
- [8] D. Leśniak, M. Bronicki, A. Woznicki, High-temperature homogenization of AlCuMg alloys for extrusion in T5 temper. *Archives of Metallurgy and Materials* **55**, 2, 499-513 (2010).
- [9] T. Shepard, On the Relationship between Extrusion Conditions, Mechanical Properties and Surface Acceptability in Some Hard Aluminum Alloys. Proceedings of the 7th International Aluminum Extrusion Technology Seminar ET'2000, Chicago, USA, 307-320 (2000).
- [10] X.J. Xu, S.S. Kim, Y.S. Zheng, Improvement in Strength of 2024 Al Alloy by Enhanced Solution Treatment. *Key Engineering Materials* **297-300**, 2362-2367 (2005).
- [11] PN-EN 573-3: 2007 – Aluminium and aluminium alloys. Chemical composition and products plastically deformed (Polish and European standard).
- [12] PN-EN 755-2: 2008 – Aluminium and aluminium alloys. Rods, tubes and profiles extruded – Part 2 (Polish and European standard).